

Article

Xyloplax princealberti (Asteroidea, Echinodermata): A New Species That Is Not Always Associated with Wood Falls [†]

Cheyenne Y. Payne ^{1,2,‡}, Ekin Tilic ^{3,‡}, Rachel E. Boschen-Rose ^{4,5}, Amanda Gannon ¹, Josefin Stiller ⁶, Avery S. Hiley ¹, Benjamin M. Grupe ⁷, Christopher L. Mah ⁸ and Greg W. Rouse ^{1,*}

¹ Scripps Institution of Oceanography, University of California San Diego, La Jolla, CA 92093, USA; cyanceypayne@gmail.com (C.Y.P.)

² Biology Department, Stanford University, Stanford, CA 94305, USA

³ Department of Marine Zoology, Senckenberg Research Institute and Natural History Museum, 60325 Frankfurt, Germany; ekin.tilic@senckenberg.de

⁴ Department of Biology, University of Victoria, Victoria, BC V8P 5C2, Canada

⁵ Marine Directorate of the Scottish Government, Aberdeen AB11 9DB, UK

⁶ Centre for Biodiversity Genomics, University of Copenhagen, 2100 Copenhagen, Denmark; josefin.stiller@bio.ku.dk

⁷ School of Earth and Ocean Sciences, University of Victoria, Victoria, BC V8P 5C2, Canada; ben.grupe@gmail.com

⁸ Department of Invertebrate Zoology, Smithsonian National Museum of Natural History, NHB-163, Smithsonian Institution, Washington, DC 20560, USA

* Correspondence: grouse@ucsd.edu

† urn:lsid:zoobank.org:pub:4414A5AF-B18F-4D8E-8FFE-E1F56C160534.

‡ These authors contributed equally to this work.

Abstract: *Xyloplax* is a genus of three species of sea stars previously found only on sunken wood in the deep ocean. Their circular and petaloid bodies, which lend them their common name “sea daisy”, and their presumed exclusive diet of wood make them an unusual and rare element of deep-sea ecosystems. We describe here the fourth species of *Xyloplax* from the eastern Pacific Ocean, *Xyloplax princealberti* n. sp., which ranges from offshore Canada to the Gulf of California (Mexico) and Costa Rica. Though sampled geographically close to another described species of *Xyloplax* from the northeastern Pacific, *X. janetae*, this new species is unique morphologically and according to available DNA data. The short abactinal spines are the most obvious feature that distinguishes *X. princealberti* n. sp. from other *Xyloplax*. The minimum distance for mitochondrial cytochrome c oxidase subunit I from *Xyloplax princealberti* n. sp. to the only other available *Xyloplax*, *X. janetae*, was 13.5%. We also describe *Ridgeia vestimentiferan* tubeworm bushes from active hydrothermal vents as a new *Xyloplax* habitat, the first record of a non-wood substrate, and a new reproductive strategy, simultaneous hermaphroditism, for this genus. We generated the first mitochondrial genome for a member of *Xyloplax* and analyzed it with other available asteroid data using nucleotide-coding or amino acid (for protein-coding genes) plus nucleotide coding (for *rRNA* genes). The nucleotide-coding results place *Xyloplax* as part of the clade Velatida, consistent with a previous phylogenomic analysis that included *Xyloplax princealberti* n. sp. (as *Xyloplax* sp.), though the placement of Velatida within Asteroidea differed. The amino acid plus nucleotide coding recovered Velatida to be a grade with *X. princealberti* n. sp. as sister group to all other Asteroidea.

Keywords: deep sea; asteroid; hydrothermal vent



Citation: Payne, C.Y.; Tilic, E.; Boschen-Rose, R.E.; Gannon, A.; Stiller, J.; Hiley, A.S.; Grupe, B.M.; Mah, C.L.; Rouse, G.W. *Xyloplax princealberti* (Asteroidea, Echinodermata): A New Species That Is Not Always Associated with Wood Falls. *Diversity* **2023**, *15*, 1212. <https://doi.org/10.3390/d15121212>

Academic Editors: Quentin Jossart and Camille Moreau

Received: 7 November 2023

Revised: 8 December 2023

Accepted: 8 December 2023

Published: 12 December 2023



Copyright: © 2023 by the authors. Licensee MDPI, Basel, Switzerland. This article is an open access article distributed under the terms and conditions of the Creative Commons Attribution (CC BY) license (<https://creativecommons.org/licenses/by/4.0/>).

1. Introduction

Xyloplax is a genus of small, deep-sea benthic asteroids that, until now, have only been known to reside on sunken wood. These are discoid in shape with short spines present around their circumference, lending them their common name “sea daisy” [1–4]. Owing to their small size (~1 cm diameter or less) and occurrence in the deep sea, very little is

known about these animals, including details about their digestive mechanism, dispersal, and reproductive strategies.

The first recorded *Xyloplax* species, *X. medusiformis*, was described in 1986 by Baker et al. [1], found in the Tasman Sea off the South Island of New Zealand at 1057–1208 m depth, and the second, *X. turnerae*, was described two years later, found on the east coast of Andros Island, Bahamas, at 2066 m [2]. The third and most recently described species, *X. janetae*, was described in 2006, found in the northeastern Pacific Ocean offshore Oregon, US, at 2675 m [2,3]. These animals were regarded to be so different morphologically from other echinoderms that, initially, both Baker et al. [1] and Rowe et al. [2] placed *Xyloplax* in its own monogeneric class called Concentricycloidea. The phylogenetic placement of Concentricycloidea has since been controversial. However, molecular data largely support that Concentricycloidea belongs within Asterozoa [3,5–7]. The most recent phylogenetic placement for *Xyloplax* based on asteroid transcriptomes is within velatid asteroids [8]. The sporadic distribution of *Xyloplax* and the general challenges of collecting samples in the deep sea have made it difficult to evaluate their range and ecology; however, both opportunistic and deployed wood collections have allowed us to sample several populations along the Pacific coast of North and Central America. Here, we present a new species of sea daisy, *Xyloplax princealberti* n. sp., which is only the fourth described *Xyloplax* species, the second described from the northeastern Pacific and the first described off the Pacific coast of Central America.

Xyloplax specimens were initially collected from wood blocks and bone deployed near hydrothermal vents of the Main Endeavour Field (MEF) on the Juan de Fuca Ridge off Canada at a depth of 2200 m, a locale ~607 km north of the type locality for *X. janetae*. Vestimentiferan tubeworm bushes from hydrothermal vents nearby, with no apparent wood substrate, also yielded specimens. Molecular and morphological data supporting the new species status for these individuals are presented here, confirming that a previously published *Xyloplax* sp. transcriptome belongs to this species [8]. Additional specimens collected from wood off the Pacific coast of Costa Rica and Mexico are also assigned to this new species. Finally, we describe simultaneous hermaphroditism as a new reproductive mode for this group.

2. Materials and Methods

2.1. Sample Collection

Xyloplax were collected off the Pacific coasts of Canada, Mexico, and Costa Rica. Specimens were collected from near the base of Hulk Chimney, Main Endeavour Field (MEF), within the Endeavour Hydrothermal Vents Marine Protected Area in Juan de Fuca Ridge, off the coast of Canada. More than 20 individuals were collected from three-year-old wood and bone deployments recovered by Deep Submergence Vehicle (DSV) *Alvin* and Research Vessel (RV) *Atlantis* on dives AD4622 and AD4627, on 11 and 20 July 2010, respectively (Figure 1A,E), located at 2201 m at 47.948° N, 129.099° W. Specimens were fixed in 10% formalin in seawater, 4% paraformaldehyde in sodium phosphate buffer (PFA), RNAlater, or 95% ethanol. Twenty-five individuals were retrieved from a *Ridgeia piscesae* tubeworm bush located on basalt at 2195 m at 47.950° N, 129.097° W, 0.21 km north of the initial samples (Figure 1B), on 9 August 2016 by CCGS *Tully* using the Remotely Operated Vehicle (ROV) ROPOS dive R1939. The clump of tubeworms and associated fauna was placed in a sealed biobox, with minimal loss of material. Material was sieved with 1 mm and 64 µm sieves, with *Xyloplax* retained on the 1 mm sieve with other tubeworm-associated macrofauna and fixed in 95% ethanol. The tubeworm surface area of the sample was determined by measuring the cylindrical area of tube images, giving macrofaunal densities per decimeter squared. Eight individuals (Figure 1F) were collected from a piece of wood (Figure 1C) found at a depth of 2421 m on the Alarcón Rise, Gulf of California, Mexico, 23.550° N, 108.418° W, by ROV *Doc Ricketts* and R/V *Western Flyer* on dive D398, 27 April 2012, and fixed in 95% ethanol. Finally, two individuals (Figure 1G,H) were collected by DSV *Alvin* and RV *Atlantis* on dive 4972, 18 October 2018, from an 18-month-old wood

deployment (Figure 1D) located at a depth of 1845 m at 9.115° N, 84.836° W, near methane seeps at Jaco Scar, offshore Costa Rica, and they were fixed in 95% ethanol. Specimens are stored at the Benthic Invertebrate Collection, Scripps Institution of Oceanography, La Jolla, California (SIO-BIC); the Royal BC Museum, Victoria, British Columbia, Canada (RBCM); la Colección Regional de Invertebrados Marinos, Estación Mazatlán UNAM (EMU), Instituto de Ciencias del Mar y Limnología, Universidad Nacional Autónoma de México, Mazatlán, Sinaloa, Mexico (ICML-UNAM); el Museo de Zoología (Universidad de Costa Rica), San José, Costa Rica (MZUCR); and Naturmuseum Senckenberg, Frankfurt, Germany (SMF).

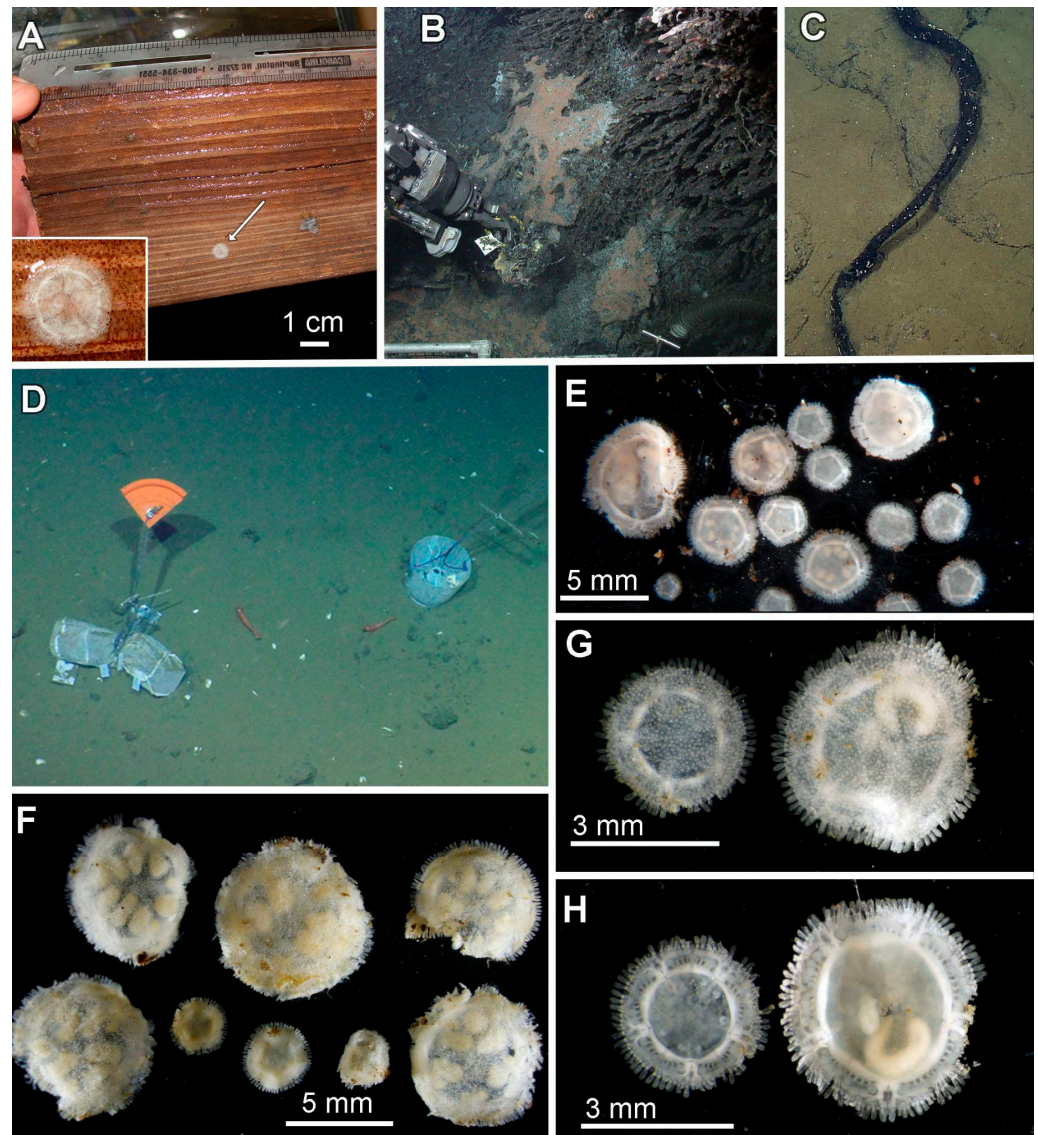


Figure 1. Collection sites and representative individuals of *Xyloplax princealberti* n. sp. (A) Recovered wood block from Juan de Fuca Ridge, offshore Canada, showing a specimen on the surface (indicated with white arrow). Inset shows an animal in situ on the wood surface. (B) *Ridgeia* vestimentiferan bush sampled at the Juan de Fuca Ridge, offshore Canada. (C) Wood found with seven specimens of *Xyloplax princealberti* n. sp. at 2421 m on the Alarcón Rise, Gulf of California, Mexico. (D) Wood deployment at 1845 m at Jaco Scar, offshore Costa Rica. (E) Specimens in abactinal view collected from wood deployment in the Juan de Fuca Ridge, offshore Canada. (F) Specimens in abactinal view collected from wood in the Gulf of California, Mexico. (G) Two specimens in abactinal view from Jaco Scar, offshore Costa Rica. (H) Two specimens in actinal view from Jaco Scar, offshore Costa Rica.

2.2. Molecular Sampling, DNA Extraction, and PCR Amplification

Mitochondrial cytochrome c oxidase subunit I (COI) DNA was Sanger-sequenced for 13 individuals, including the holotype (SIO-BIC E11463). Internal soft tissue of each individual was dissected from the external skeleton, or the animal was bisected, and half was used for extraction. DNA was extracted and purified from the soft tissue using a Zymo Research (Irvine, CA, USA) MiniPrep or MicroPrep kit. A 650 bp region was amplified using the primers LCO1490 and HCO2198 [9] for one Canada wood specimen, two Canada *Ridgeia* tubeworm specimens, six Mexico specimens, and one Costa Rica specimen. We were unable to sequence this region for three Canada wood specimens (SIO-BIC E11165, E11166 and the holotype E11463) owing to DNA degradation, so we designed custom primers to target a 430 bp region that overlapped (in part) the LCO1490 and HCO2198 region using the COI sequence mined from the transcriptome (forward XyloF2 5'-CCAGGATTTGGCATGATTTCTCA-3', reverse XyloR2 5'-TGCAAATACAGCTCCCATGA-3'). We sequenced this shorter region for the three degraded specimens as well as the other 10 specimens. This resulted in around ~950 bp of COI for most of the specimens. One specimen collected from wood deployed off Canada had previously been used to generate a transcriptome and was published as *Xyloplax* sp. [8], with specimen voucher SIO-BIC E6809. The SRA data (SRR2846120) were mined for a 1223 bp fragment COI sequence (see below). A total of 14 COI sequences, including that mined from the transcriptome, were deposited on NCBI GenBank under accession numbers OR730451–OR730463 and OR915671 (the holotype).

2.3. Mitochondrial Genome Sequencing and Assembly

DNA was extracted from a specimen collected from Mexico (MZUCR-ECH2401, formerly SIO-BIC E11453) using the Zymo Research (Irvine, CA, USA) DNA-Tissue Miniprep kit. DNA quantity was estimated using a Qubit dsDNA BR Assay Kit with a Qubit fluorometer (Invitrogen, Waltham, MA, USA) and fragment size was checked with agarose gel electrophoresis. Library preparation and sequencing were carried out by Novogene Corporation Inc. (Sacramento, CA, USA). Animal whole-genome libraries were prepared, targeting an insert size of 350 bp. A total of 11,180,866 paired-end reads (150 bp) were sequenced on an Illumina NovaSeq 6000 (San Diego, CA, USA).

The complete circular mitochondrial genome was assembled with GetOrganelle v1.7.5.2 [10], which uses a “baiting and iterative mapping” approach to de novo assemble circular organelle genomes with Bowtie2 [11] and SPAdes [12]. The average base coverage for the assembly was 78.2x with a minimum coverage of 32x. The assembled mitochondrial genome was first annotated on the MITOS2 web server (RefSeq 81 Metazoa; Genetic Code 9) [13] and then manually confirmed with Geneious Prime[®] 2022.0.1. In addition to the specimen from Mexico (SIO-BIC E11453), mitochondrial genes were also mined from the published transcriptome of *X. princealberti* n. sp. (SIO-BIC E6809). The raw RNAseq reads were downloaded from NCBI (SRR2846120). Sequence adapters and low-quality regions were removed using Trimmomatic v.0.36 [14] with default parameters. Trimmed reads were assembled using Trinity [15]. Published mitochondrial genomes of Asteroidea were used as queries to identify transcripts with mitochondrial sequences. The raw reads and the mitogenome were deposited in GenBank under the accession numbers PRJNA1032079 and OR818549, respectively.

2.4. Phylogenetic and Haplotype Network Analyses

Relationships between individuals collected from the three sampled sites and *Xyloplax janetae* were evaluated using the COI sequences. Currently, no COI sequences are available for the other two species in this genus, *X. medusifformis* and *X. turnerae*. A partial 18S sequence is available for *X. turnerae* (GenBank accession AH008333). However, this sequence's BLAST is closest to several ophiuroids, instead of the expected *X. janetae* 18S sequence, suggesting that the sequence may be an error. COI sequences for *X. janetae* and three other members of Velatida were downloaded from GenBank (see accession

numbers on Figure 2) into Mesquite v3.61 [16], and aligned with MAFFT v7.490 [17]. A maximum-likelihood (ML) analysis was performed using RAxML GUI v 2.0 [18] RAxML-NG [19] applying the GTR+GAMMA model following assessment with ModelTest-NG v0.1.7 [20] with 100 random searches, with support assessed via thorough bootstrapping (with 1000 pseudo-replicates).

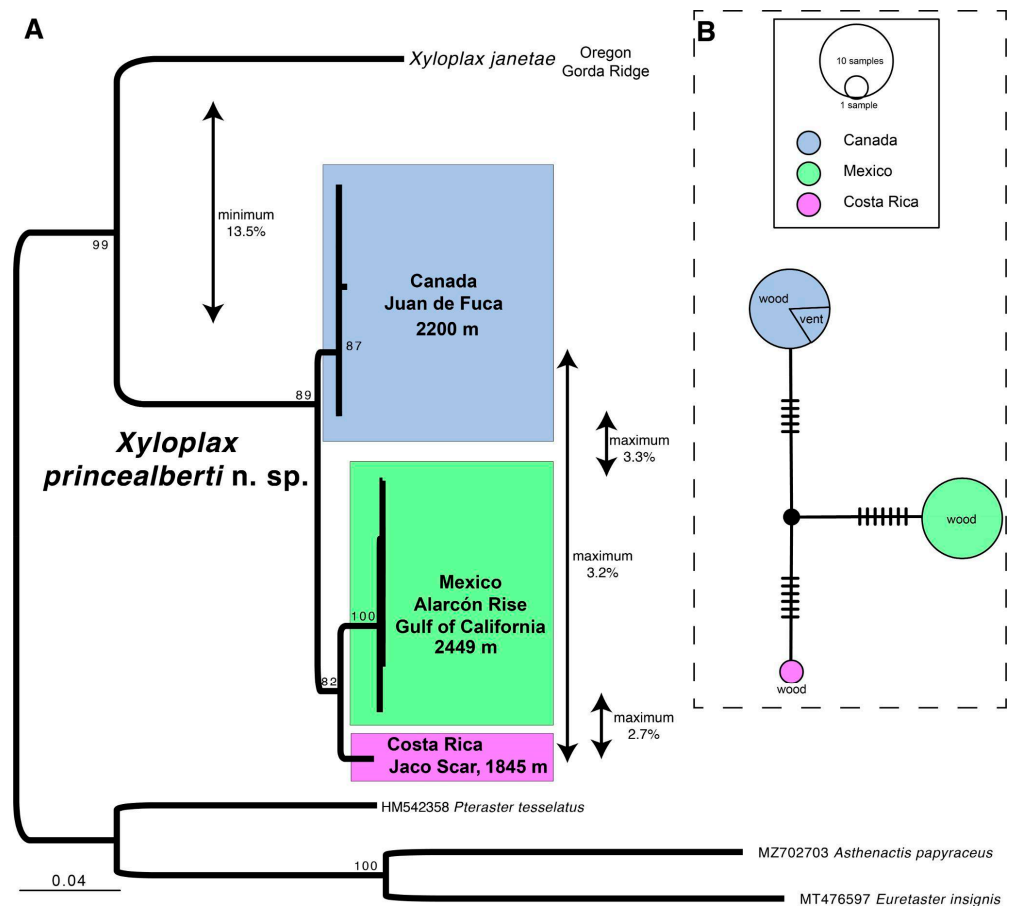


Figure 2. Analysis of mitochondrial COI data. (A) Maximum-likelihood analysis of COI for all sequenced *Xyloplax princealberti* n. sp. specimens, as well as the only available other COI sequence for a *Xyloplax*, *X. janetae*. Other members of Velatida were used as the outgroup. The minimum distance from *X. janetae* to *X. princealberti* n. sp. is 13.8%. Within *Xyloplax princealberti* n. sp., the single Costa Rica specimen groups with Mexico specimens are sister to the Canadian population. The maximum distance found among all the *X. princealberti* n. sp. specimens is 3.3%. (B) TCS haplotype network for 12 individuals of *X. princealberti* n. sp. based on a 354 bp COI alignment. Note that the Canadian samples collected from both wood and tubeworms (vent) showed the same haplotype.

Uncorrected pairwise COI distances among *X. princealberti* n. sp. specimens and with *X. janetae* were calculated using PAUP* v4a168 [21]. Relationships among the sequences, site (Canada, Mexico, Costa Rica), and habitats (wood, vents) were visualized with a TCS [22] haplotype network generated using PopArt [23]. This was based on a 354 bp alignment that had no missing data.

The mitogenome of *X. princealberti* n. sp. was analyzed with a range of other available mitochondrial genomes for Asteroidea using RAxML-NG. Other terminals, including ophiuroid outgroups, were sourced from two recent studies on asteroid mitogenomics [24,25], with accession numbers shown in Figure 3. The two RNA genes were analyzed with the 13 protein-coding genes (PCGs), which were coded as either DNA or as amino acids, resulting in two analyses. Models for each of the 15 concatenated partitions for each analysis were selected using ModelTest-NG v0.1.7. For the all-DNA analysis, the models were

as follows: 12S = GTR+I+G, 16S = TIM3+I+G, ATP6 = TIM2+I+G, ATP8 = TPM2uf+I+G, COI = TVM+I+G, COII = TIM2+I+G, COIII = TIM2+G, CytB = GTR+I+G, ND1 = GTR+I+G, ND2 = GTR+I+G, ND3 = TIM2+I+G, ND4 = TIM2+I+G, ND4L = TPM2uf+I+G, ND5 = GTR+I+G, and ND6 = GTR+I+G. For the analysis with PCGs as amino acids, the RNA genes were still coded as DNA with the same models as all DNA analysis, but the amino acid models were as follows: ATP6 = MTZOA, ATP8 = MTREV, COI = MTZOA, COII = MTZOA, COIII = MTZOA, CytB = MTZOA, ND1 = MTZOA, ND2 = MTZOA, ND3 = MTREV, ND4 = MTZOA, ND4L = MTREV, ND5 = MTREV, and ND6 = HIVB. ML searches were conducted with 10 random searches and support was assessed via thorough bootstrapping with 100 pseudoreplicates. Since the nucleotide and amino-acid-translated datasets produced slightly different topologies regarding the placement of *X. princealberti* n. sp. and the monophyly of Velatida, an approximately unbiased (AU) test [26] was conducted on the amino acid plus nucleotide dataset to assess if the likelihood of a paraphyletic Velatida was significantly better than a monophyletic Velatida. A constrained tree-forcing monophyly of Velatida was made using Mesquite and RAxML-NG. The AU test was conducted in IQ-Tree v.1.6.12 [27] with 20,000 replicates to generate likelihood scores and *p*-values for the constrained and unconstrained (ML nucleotide-only) trees.

2.5. Morphology

Specimens were photographed with a Leica MZ9.5 or 12.5 stereomicroscope with a Canon Rebel T3i camera. We took SEM images of the skeletal structures of two Canadian specimens preserved in 95% ethanol, including the adambulacral spines, abactinal plates, and actinal and abactinal surfaces (part of lots E11163 and E11164). Another Canadian specimen (SIO-BIC E11159) had all tissue dissolved in bleach to leave the skeletal elements. These were rinsed and dehydrated in ethanol and HMDS, air-dried, and coated in gold palladium. Specimens were imaged using either a Zeiss EVO10 or a Hitachi S4800 scanning electron microscope operating at 20 kV or 5 kV, respectively.

One Mexican specimen (SMF 6936) preserved in 95% ethanol was scanned using a Werth (Giessen, Germany) Tomoscope[®] XS Plus 200 microCT with the following scan parameters: 85 kV voltage, 188 μ A generator current, and 16 W generator power. Exposure time was 666 ms with a total of 2700 projections (3 projections were averaged). The voxel resolution was 3.56 μ m. Surface renderings were generated with the software Drishti v3.1 (National University, Canberra, Australia) [28]. The raw microCT dataset, together with the surface renderings, is deposited online as a cybertype: <https://doi.org/10.5281/zenodo.10042987> (accessed on 26 October 2023).

Canadian specimens fixed in paraformaldehyde (4%) in 0.2 M sodium phosphate buffer with 0.3 M sucrose added were left in the fixative for several months, which resulted in decalcification. Some of the specimens were embedded in Spurr's resin and one (SIO-BIC E11155) was sectioned at 1 μ m thickness with a Power Tome X. The sections were stained with Toluidine Blue and imaged with an EOS Rebel T6i on a Leica (Wetzlar, Germany) DMR compound microscope.

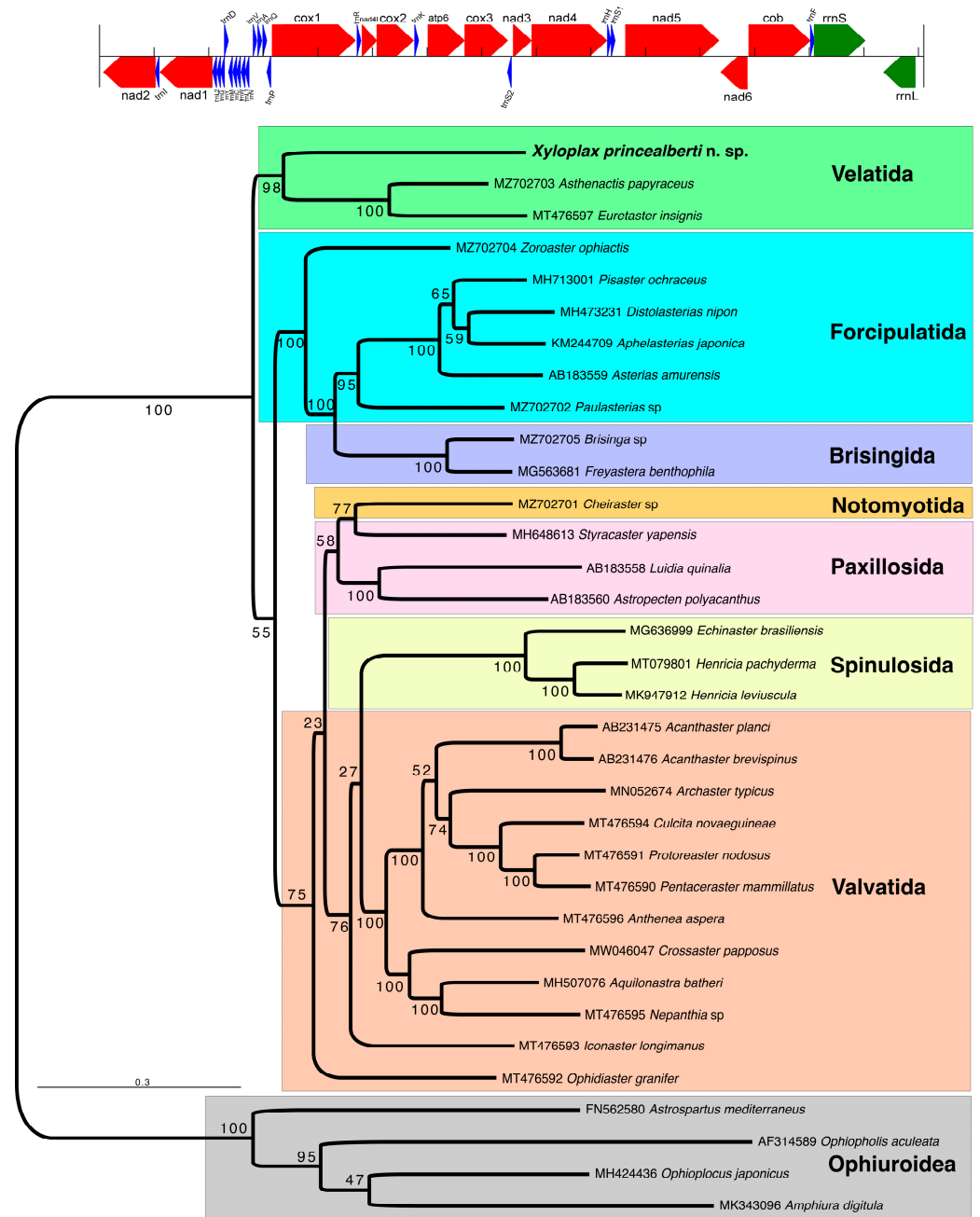


Figure 3. Mitochondrial genome order of *Xyloplax princealberti* n. sp. and maximum-likelihood phylogenetic tree. The top schematic shows the gene order of the mitogenome of *X. princealberti* n. sp., which is identical to that recovered for all other Asterozoa [24,25]. The bottom panel shows the maximum-likelihood phylogeny built from the 15-gene dataset with all partitions encoded as DNA. *X. princealberti* n. sp. is in a well-supported Velatida clade, which is supported as the sister group to all other Asterozoa. A second analysis with PCGs encoded as amino acids recovered Velatida as a grade with *X. princealberti* n. sp., sister to a poorly supported clade of all other Asterozoa, but the topology was otherwise largely the same as that shown here (Supplementary Figure S1).

3. Results

3.1. Species Delimitation

The maximum-likelihood tree of COI sequences (Figure 2A) shows that the Canadian wood deployment and tubeworm individuals and the wood-dwelling Mexico and Costa Rica individuals group to form a clade with 89% support as a sister taxon to *Xyloplax janetae*.

This clade has a minimum uncorrected divergence of 13.5% from *X. janetae*; therefore, we describe this group as *X. princealberti* n. sp. (Figure 2A). Within *X. princealberti* n. sp., there is a maximum 3.3% uncorrected pairwise distance between individuals from the Canada (type locality) and Mexico populations, 3.2% between Canada and Costa Rica, and 2.7% between Mexico and Costa Rica (Figure 2A). The haplotype network analysis of a 354 bp COI sequence revealed that the Canadian, Mexican, and Costa Rican populations have unique haplotypes (Figure 2B). Notably, despite their association with unique substrates, individuals collected from wood and *Ridgeia* tubeworms in the same vent system in offshore Canada share the same haplotype for this sequence (Figure 2B).

3.2. Assembled Mitochondrial Genome

The complete mitochondrial genome of *Xyloplax princealberti* n. sp. was 19,663 bp in length. In total, 13 protein-coding genes (PCGs), 22 *tRNAs*, and 2 *rRNAs* were identified. The GC content is 24.8% (38.6% A, 9.9% G, 14.9% C, 36.6% T). The recovered gene order (Figure 3) matches that of other published Asteroidea. *ND1* and *ND4L* have the start codon TTG, as previously described only in *Euretaster* [24], and *ND3* has the start codon ATT, while all the other PCGs have the start codon ATG. The stop codon for *ND4*, *ND3*, and *ND1* is TAG; for all other PCGs, the stop codon is TAA. The average divergence between all PCGs mined from the transcriptome (SIO-BIC E6809 from Canada, type locality) and those from the genome-skimmed specimen (SIO-BIC E7655 from Mexico) was ~2.85%. The highest divergence was 3.9% for ATP6 and lowest were the two *rRNAs* with 0.5% for the partial 16S and 1.9% for 12S.

3.3. Phylogenetic Placement of *Xyloplax* in Asteroidea

The analysis with 15 PCGs encoded as nucleotides (Figure 3) placed *X. princealberti* n. sp. within a well-supported Velatida clade (bootstrap 98), a sister group to all other Asteroidea. The analysis with 13 PCGs encoded as amino acids and two RNA genes encoded as nucleotides showed a similar topology, but *X. princealberti* n. sp. was recovered as a sister group to a poorly supported clade of all other Asteroidea, with Velatida forming a grade (Figure S1). We tested the significance of this placement in the amino acid tree using an AU test, where a monophyletic Velatida (including *X. princealberti* n. sp.) was enforced as a constraint. The constrained best tree and the best tree were not significantly different ($p = 0.262$).

3.4. Ecological Observations

Specimens were found on wood at all three sites. Individuals from the Canada and Costa Rica wood deployments were alive upon recovery. Some individuals from the Canadian wood deployment showed minor spine movement, though no locomotion was observed. *Xyloplax princealberti* n. sp. were also recovered from a *Ridgeia piscesae* tubeworm bush at an active hydrothermal vent (Figure 1A). The density of individuals over the whole tubeworm bush was 0.57 dm^{-2} . The tubes of *R. piscesae* that were sampled were generally long (max tube length 82 cm), with relatively small diameters (max tube width 0.6 cm) and few flanges. The bush architecture was loose, although the tubeworms' lower trunks ("roots") had a more complex interlocking structure. Some tubes showed evidence of external metal oxide deposition. Few *R. piscesae* branchial plumes were visible prior to sampling. The long, narrow tubes alongside metal oxide deposition and few visible branchial plumes suggest that this *R. piscesae* bush was in a relatively low hydrothermal flow regime, with hydrothermal fluid either coming overhead from the Hulk Chimney close behind or through cracks in the basalt below. Temperature within the bush was 2–4 °C (mean 3 °C), which was slightly elevated compared to the background temperature of 2.2 °C; faintly shimmering water was visible directly above the tubeworm bush. There was a fair amount of detritus collected with the tubeworm sample, which seemed to largely consist of degraded *R. piscesae* tubes; this material may have been retained in situ by the complex interlocking tube structure towards the base of the bush. The macrofaunal assem-

blage of *R. piscesae* samples largely consisted of species typically found at low-temperature, basalt-hosted hydrothermal vents in the region; 97.76% of the individuals from the assemblage could be considered vent-endemic. Non-vent species more associated with the vent periphery were also found (0.46% of individuals), such as benthic forams, cladorhizid sponges, and hydroids, indicating that the macrofaunal assemblage at this site includes some opportunistic deep-sea species. *Xyloplax princealberti* n. sp. specimens comprised 1.77% of individuals found in the *R. piscesae* bush sampled, and this was the seventh most abundant taxon among the macrofauna. Of the 23 macrofaunal taxa identified, 19 are considered vent-endemic. *Xyloplax* occurred in greater abundance than 13 of these taxa.

3.5. Taxonomy

VELATIDA

XYLOPLACIDAE Baker, Rowe & Clark, 1986 [1]

Xyloplax Baker, Rowe & Clark, 1986 [1]

Xyloplax Baker, Rowe & Clark 1986: 862; Rowe, Baker & Clark 1988: 455; Mah 2006: 142 [1–3]

Ankyloplax Gale, 2011 [29], new synonym

Xyloplax princealberti n. sp.

Xyloplax sp. Linchangco et al. 2017: 166, 168 [8]

3.6. Material Examined

Holotype: SIO-BIC E11463 (fixed in ethanol and the velum and gonads used for DNA extraction), on wood deployment at 2201 m near Hulk Chimney, Main Endeavour Field, Juan de Fuca Ridge, Canada, 47.948° N, 129.099° W, 20 July 2010, DSV *Alvin* dive 4627, collectors Kirt Onthank and Kiana Frank, GenBank: OR915671 (COI). Paratypes: SIO-BIC E6809 (seven specimens fixed in seawater formalin and preserved in 50% ethanol; one fixed in RNA later and destroyed for transcriptome sequencing), collection locality same as holotype, 11 July 2010, DSV *Alvin* dive 4622, collectors Ben Grupe and Heather Olins, GenBank: OR730458 (COI); SIO-BIC E11155 (five specimens fixed in paraformaldehyde and embedded in resin, of which one was partially sectioned onto microscope slides; one specimen fixed in paraformaldehyde and preserved in 50% ethanol), collection details same as holotype (DSV *Alvin* dive 4627); SIO-BIC E11156 (three specimens and juveniles, fixed in seawater formalin and preserved in 50% ethanol), collection details same as E6809 (DSV *Alvin* dive 4622); SIO-BIC E11157 (three specimens and juveniles, fixed and preserved in 95% ethanol), collection details same as E6809 (DSV *Alvin* dive 4622) except substrate was bone, not wood; SIO-BIC E11158 (six specimens and juveniles, fixed in seawater formalin and preserved in 50% ethanol), collection details same as E6809 (DSV *Alvin* dive 4622); SIO-BIC E11159 (one specimen fixed in ethanol, dissociated in bleach, dried, and mounted on two SEM stubs), collection details same as E6809 (DSV *Alvin* dive 4622); SIO-BIC E11160 (one specimen fixed and preserved in 95% ethanol), collection details same as E6809 (DSV *Alvin* dive 4622); SIO-BIC E11162 (one specimen fixed in seawater formalin and then 3% glutaraldehyde, rinsed, and preserved in 50% ethanol), collection details same as E6809 (DSV *Alvin* dive 4622); SIO-BIC E11163 (ten specimens fixed and preserved in 95% ethanol, of which one specimen was dried and mounted on an SEM stub), collection details same as E6809 (DSV *Alvin* dive 4622); SIO-BIC E11164 (eight specimens fixed and preserved in 95% ethanol, of which two were dried and mounted on SEM stubs; one specimen fixed in seawater formalin and preserved in 50% ethanol), collection details same as E6809 (DSV *Alvin* dive 4622) except substrate was bone, not wood; SIO-BIC E11170 (one specimen fixed and preserved in 95% ethanol), in *Ridgea piscesae* tubeworm bush at 2195 m near Hulk Chimney, Main Endeavour Field, Juan de Fuca Ridge, Canada, 47.950° N, 129.097° W, August 9, 2016, ROV *ROPOS* dive R1939, collector Rachel Boschen-Rose, GenBank: OR730463 (COI); SIO-BIC E11171 (one specimen fixed and preserved in 95% ethanol), same collection details as E11170, GenBank: OR730462 (COI); SIO-BIC E11172, E11173, E11174, E11175, E11176, E11177, E11178 (each specimen fixed and preserved in

95% ethanol), collection details same as E11170; RBCM 023-00063-001, (five specimens fixed and preserved in 95% ethanol; was part of SIO-BIC E11461), collection details same as SIO-BIC E11170; SIO-BIC E7224 (one specimen fixed in paraformaldehyde and post-fixed in osmium tetroxide; one specimen fixed in ethanol and destroyed for DNA sequencing), on wood deployment at 1845 m, Jaco Scar, Costa Rica, 9.1146° N, 84.8356° W, 18 October 2018, DSV *Alvin* dive 4972, collectors Greg Rouse and Avery Hiley, GenBank: OR730457 (COI); SIO-BIC E7655 (one specimen fixed and preserved in 95% ethanol), on wood found at 2421 m, Alarcón Rise, Gulf of California, Mexico, 23.5505° N, 108.4183° W, 27 April 2012, ROV *Doc Ricketts* dive 398, collectors Dave Clague and Lonny Lundsten; MZUCR-ECH2401 (was SIO-BIC E11453) (one specimen fixed and preserved in 95% ethanol), collection details same as SIO-BIC E7655, GenBank: OR730455 (COI), OR818549 (mitogenome); SMF 6936 (was part of SIO-BIC E7655) (one specimen, cybertype, fixed and preserved in 95% ethanol, used for μ CT scan <https://doi.org/10.5281/zenodo.10042987> (accessed 26 October 2023)), collection details same as SIO-BIC E7655; SMF 6937 (was SIO-BIC E11454) (one specimen fixed and preserved in 95% ethanol), collection details same as SIO-BIC E7655, GenBank: OR730456 (COI); ICML-EMU-13813 (was SIO-BIC E11455) (one specimen fixed and preserved in 95% ethanol), collection details same as E7655, GenBank: OR730454 (COI); SIO-BIC E11457 (one specimen fixed and preserved in 95% ethanol), collection details same as E7655, GenBank: OR730452 (COI); SIO-BIC E11458 (one specimen fixed and preserved in 95% ethanol), collection details same as E7655, GenBank OR730451 (COI). Other material: SIO-BIC E11165 (one specimen fixed and preserved in 95% ethanol, destroyed for DNA extraction), collection details same as E6809 (DSV *Alvin* dive 4622), GenBank: OR730459 (COI); SIO-BIC E11166 (one specimen fixed and preserved in 95% ethanol, destroyed for DNA extraction), collection details same as E6809 (DSV *Alvin* dive 4622), GenBank: OR730460 (COI); SIO-BIC E11168 (one specimen fixed and preserved in 95% ethanol, destroyed for DNA extraction), collection details same as E6809 (DSV *Alvin* dive 4622), GenBank: OR730461 (COI); SIO-BIC E11462 (one specimen fixed in seawater formalin and preserved in 50% ethanol), collection details same as E6809 (DSV *Alvin* dive 4622); SIO-BIC E11456 (one specimen fixed and preserved in 95% ethanol, destroyed for DNA extraction), collection details same as E7655, GenBank: OR730453 (COI).

3.7. Diagnosis

Xyloplax with rounded abactinal spine bases, spines uniformly short. Two to three adambulacral spines per plate; more than 100 total spines around margin. Tube feet rounded, bulbous, up to ten per segment. Terminal plates badge-shaped. Mouth, gut, and anus absent. “Viviparous”, simultaneous hermaphrodite.

3.8. Description (Based on the Holotype Plus Paratypes, Where Relevant)

Body discoidal to weakly pentagonal (Figures 1D–G, 4A,B,E–G, 5 and 6). Diameter of holotype (Figure 4E–G) 2.55 mm. Paratype diameters from 1 mm to 7.6 mm. Anus absent. Abactinal plates imbricate, overlapping, irregular to round. Abactinal plates translucent. Central plate region clear but boundary visible on each plate where they overlap over one another (Figures 4A,C,E, 6A,D and 8C,D). Under SEM (when tissue present), distinct dermal layer present, covering short spinelets, plate surface, extending to peripheral spines. Under SEM (tissue partly removed), thin fibers between plates extending from stereom pores on surface (Figure 6A,B). Each plate highly porous (following tissue removal), variably shaped ranging from irregular to more quadrate in outline, some plates with jagged edges, but overall variable in size with some plates, especially the terminals 2 to 3X the size of others. (Figures 6A,B and 7A,B). Abactinal surface covered with short spinelets, 6 to 25 per plate, mostly uniform in height and size, each one slightly higher than wide, but some closer to equal height and width (Figures 4A,C,E, 6A,B and 8A,C,E,F). Hydropore present, polygonal in shape, in primary inter-radial plate (Figures 4A, 6A and 7D,E).

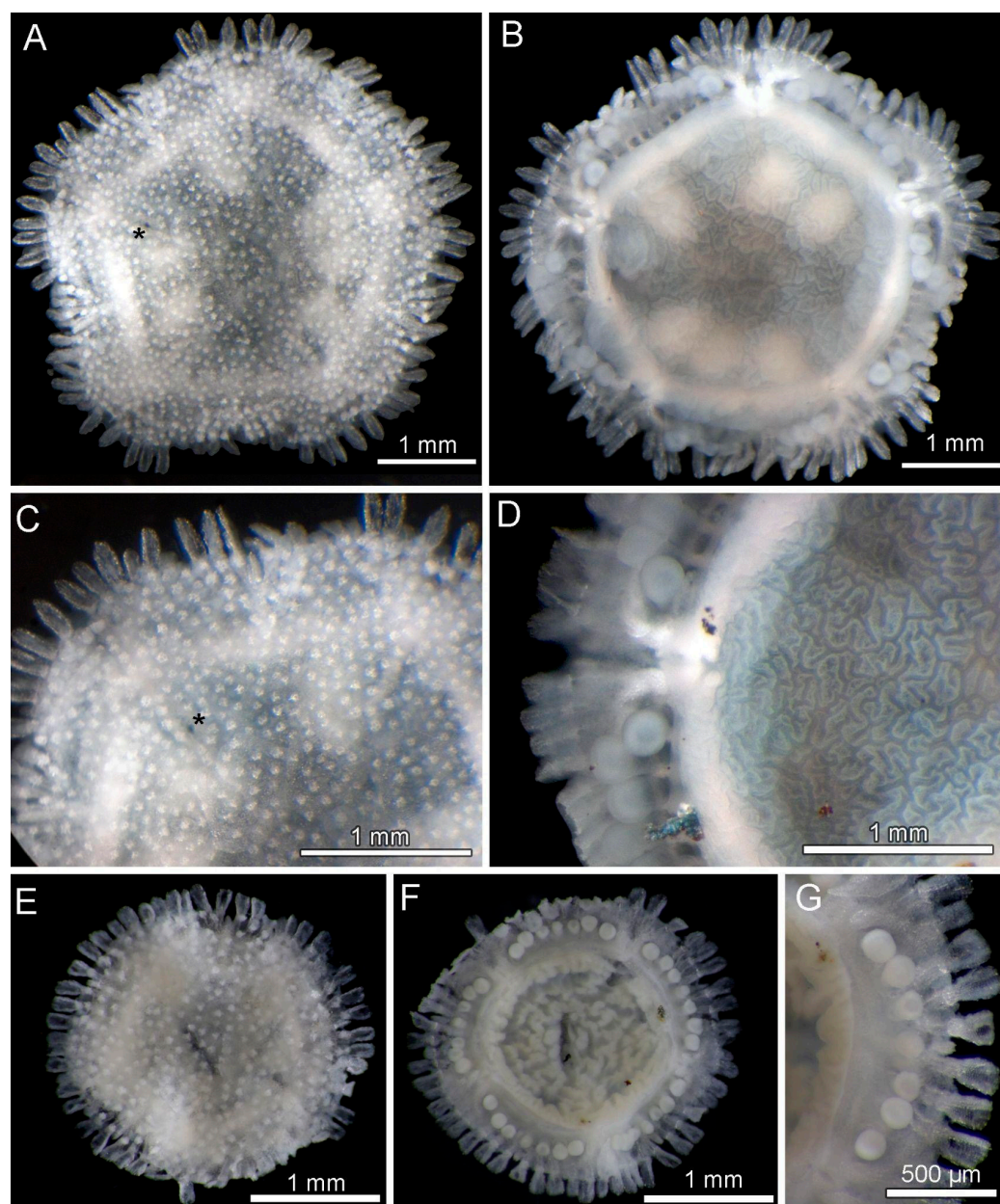


Figure 4. Images of *Xyloplax princealberti* n. sp. from the wood deployment in Juan de Fuca Ridge, offshore Canada. (A) Live specimen (from lot SIO-BIC E6809), abactinal view. * indicates hydropore. (B) Live specimen (lot SIO-BIC E6809), actinal view. (C) Closeup of the abactinal view of a live specimen (lot SIO-BIC E6809), showing adambulacral spines and short abactinal spinelets. * indicates hydropore. (D) Closeup of the actinal view of a live specimen (lot SIO-BIC E6809), showing tube feet and adambulacral spines. (E) Preserved holotype (SIO-BIC E11463), abactinal view. (F) Preserved holotype (SIO-BIC E11463), actinal view. (G) Preserved holotype (SIO-BIC E11463), closeup ambulacral area showing 7 tube feet and abactinal spinelets, abactinal view.

Abactinal spinelets composed of multi-tipped prong-like support structures around central open axis, each prong with jagged tips; 6 to 12 in total distributed on different supports, with thick rounded base, round to polygonal in outline. Support structures and the basal ring with large, open pores of variable shape and size ranging from circular to irregular in shape (Figure 7E–G). Base of each spinelet with thin fibers articulated to the underlying plate (Figure 6B). Terminal plates, badge, or “A”-shaped with blunt to rounded edges, covered by abactinal spinelets, 10–25, as described above (Figures 6A,B and 7A). Terminal plate along lower edge with discrete notch, each side flanked by two adambulacral

spines with distinct concave articulation points visible on internal surface. Stereom in the area adjacent proximal to notch and along central region with larger pores and openings relative to surrounding pores (Figure 7A).

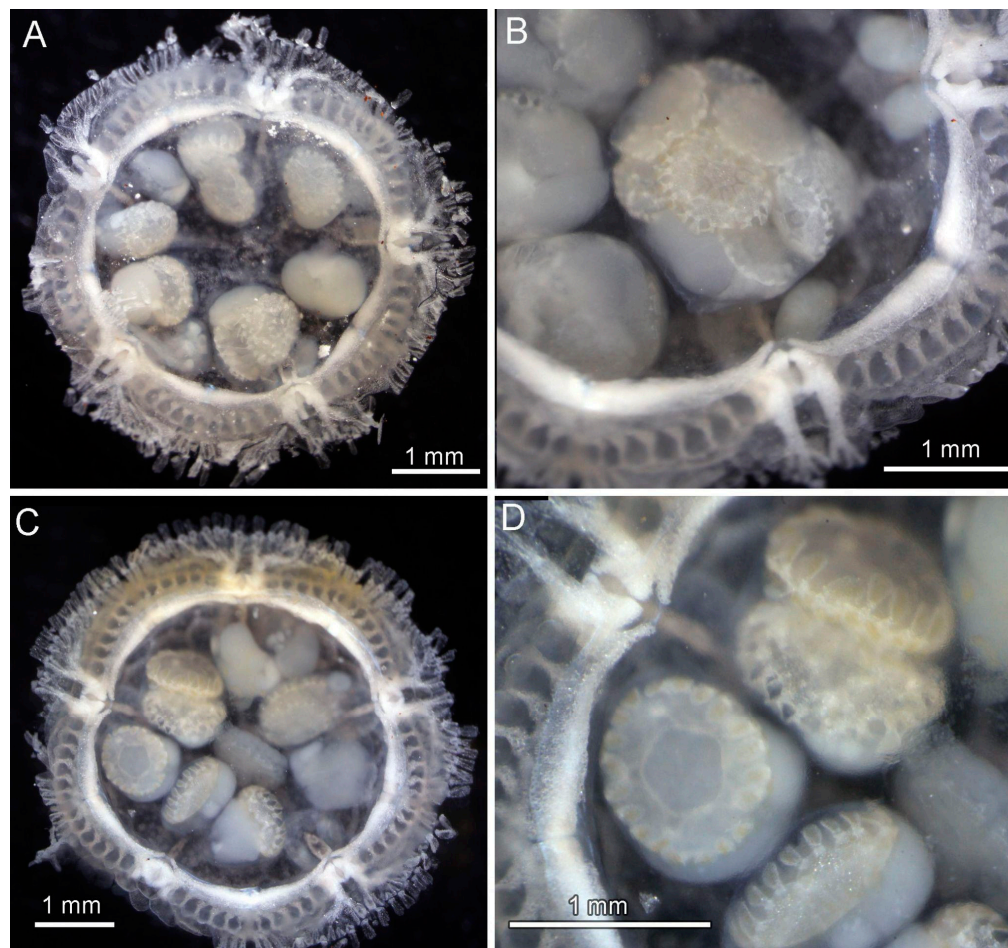


Figure 5. Images of preserved *Xyloplax princealberti* n. sp. specimens carrying developing embryos, collected from the wood deployment in Juan de Fuca Ridge, offshore Canada. (A) Actinal view of preserved specimen (SIO-BIC E11165; destroyed for DNA extraction) with velum removed to show gonads, several of which have developing embryos. (B) Closeup actinal view of preserved specimen (SIO-BIC E11165) with velum removed, showing gonads, with one containing multiple embryos. (C) Actinal view of preserved specimen (SIO-BIC E11166; destroyed for DNA extraction) with velum removed, revealing gonads. (D) Closeup of preserved specimen (SIO-BIC E11166) with velum removed, showing gonads with developing young.

Inter-radial adambulacral plates with broad, upturned, scoop-shaped spines, two to three (Figures 4A–G, 5A, 6C and 8A–F). Each spine articulated with elongated, weakly concave swelling on the terminal and other articulation adambulacral plates (Figures 4G and 7C,D). Individual adambulacral spines strongly concave in cross-section with internal curvature facing dorsally (Figure 7C,D). Length ~1.5 times width (at widest point). ~20 adambulacral spines per inter-radius = 100 total (at diameter = 3.0 mm) (Table 1). Under SEM, adambulacral spines with numerous obliquely oriented stereom pores are seen. On outward surface (convex side), numerous distinct ridges present with pointed processes directed outward and away from proximal region, approximately 10–15 serrate processes present around spine edge (Figure 7C). On inward surface (concave side), approximately two to three extended processes on spine surface with spines and jagged points towards distal end, versus more proximal region, which is devoid of projections (Figures 6B and 7D). Lateral edges along each spine, devoid of spines near base and with only 7 to 10 serrations

per side. Spine tips wide with broadly serrated edge, broken and irregular in several observed SEM images, but squarish and angular when observed as gross morphology (Figures 4, 6A–C and 7C,D). Pores on these spines more elongate and open near spinet, smaller and more homogeneous in shape near spine base. Individual adambulacral plates, flat with spines, and articulation points extending onto each plate, variably one to three. Cygnoid spinelets located inter-radially, five pairs (Figure 8C,E).

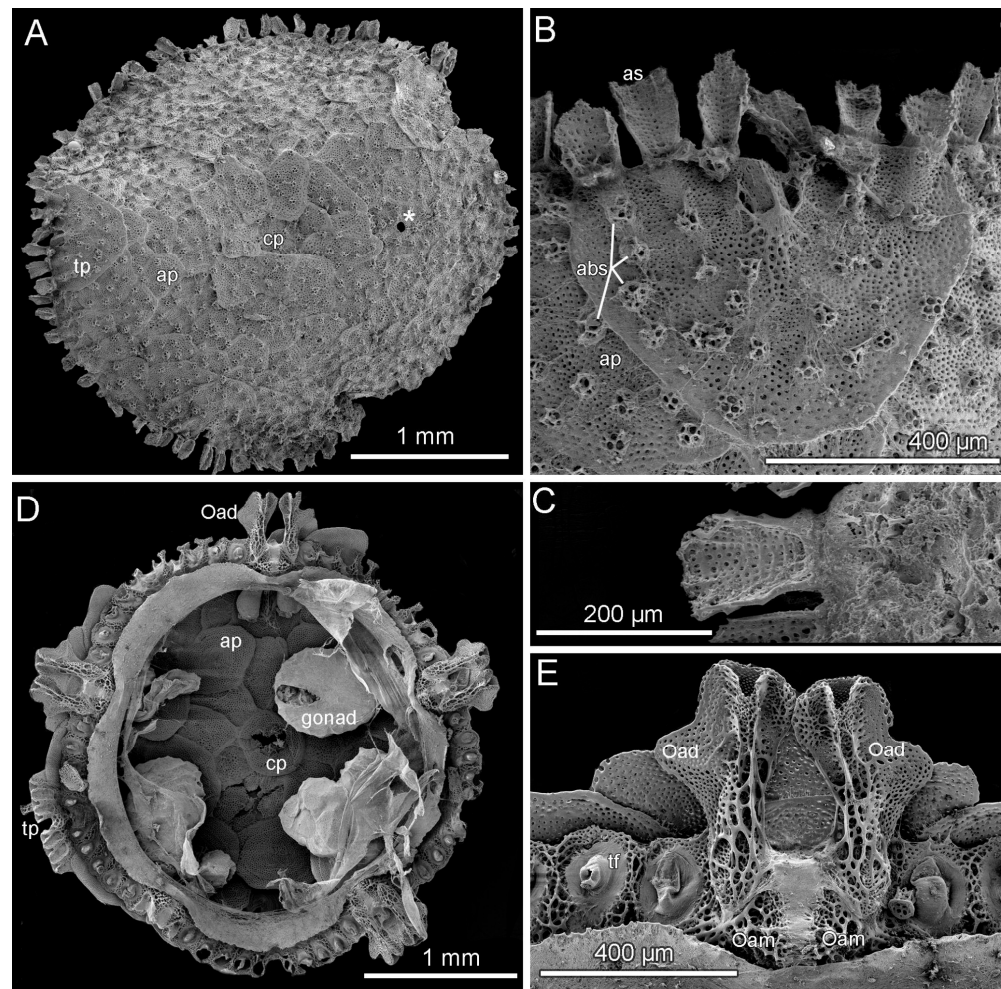


Figure 6. Scanning electron microscopy of preserved *Xyloplax princealberti* n. sp. paratypes collected from the wood deployment in Juan de Fuca Ridge, offshore Canada. No tissue was removed from individuals used. (A) Paratype SIO-BIC E11164, abactinal view showing abactinal plates and spines, madreporite, and adambulacral spines. * indicates hydropore. (B) Paratype SIO-BIC E11164 closeup abactinal view of the terminal plate, with polygonal ossicles that resemble the base of spines. (C) SIO-BIC E11164 abactinal view of adambulacral spine. (D) SIO-BIC E11163 actinal view with velum removed showing gonads and ventral surface of the abactinal plates. (E) Paratype SIO-BIC E11163 closeup actinal view of the terminal plate. Legend: **abs**: abactinal spinelet; **ap**: abactinal plate; **as**: adambulacral spine; **cp**: centrodorsal plate; **Oad**: oldest (first) adambulacral plate; **tp**: terminal plate.

Oldest ambulacral and adambulacral plates prominent, demarcating five body segments, alternating with terminal plates (Figures 4B,F, 5A,C, 6D and 8B,D). Gross morphology suggests oldest adambulacral plates have two spine articulation points (e.g., Figure 5). Under SEM, each display two prominent spines displaying wide, dorsal-facing flanges with porous stereom (Figure 6E) either side of a distinct U-shaped concavity. Basal part of this oldest adambulacral/ambulacral structure appears to be composed of two components

articulated with a tissue-filled diastema (Figure 6E). Actinal region pentagonal to weakly pentagonal in shape, as outlined by oral plates. Velum creased/wrinkled texture overlying the gonads (Figure 4B,D,F). No mouth or intestine observed. Tube feet ~10 per inter-radius (Figures 4B,D,F,G and 8B). Gonads often with developing juveniles in larger specimens (Figure 5). Semithin sections of specimen prepared for histology (Figure 9A–D) showed the presence of both ovaries (with previtellogenic and vitellogenic oocytes) and separate testes (with developing sperm).

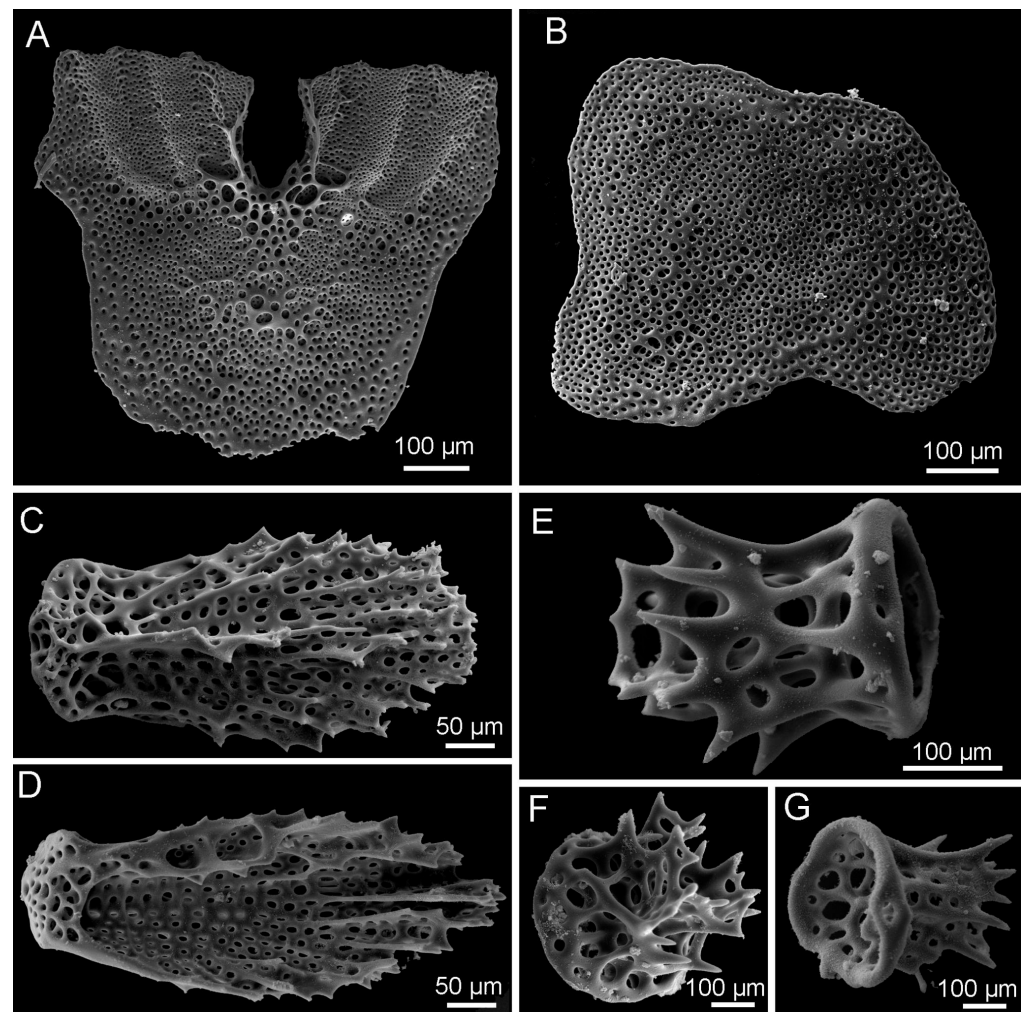


Figure 7. Scanning electron microscopy of disassociated structures from preserved *Xyloplax princealberti* n. sp. specimens collected from the wood deployment at Juan de Fuca Ridge, offshore Canada (paratype SIO-BIC E11159). (A) Terminal plate, actinal surface. (B) Abactinal plate. (C) Actinal view of adambulacral spine. (D) Abactinal view of adambulacral spine. (E) Lateral view of abactinal spinelet. (F) Abactinal view of abactinal spinelet. (G) Actinal view of abactinal spinelet.

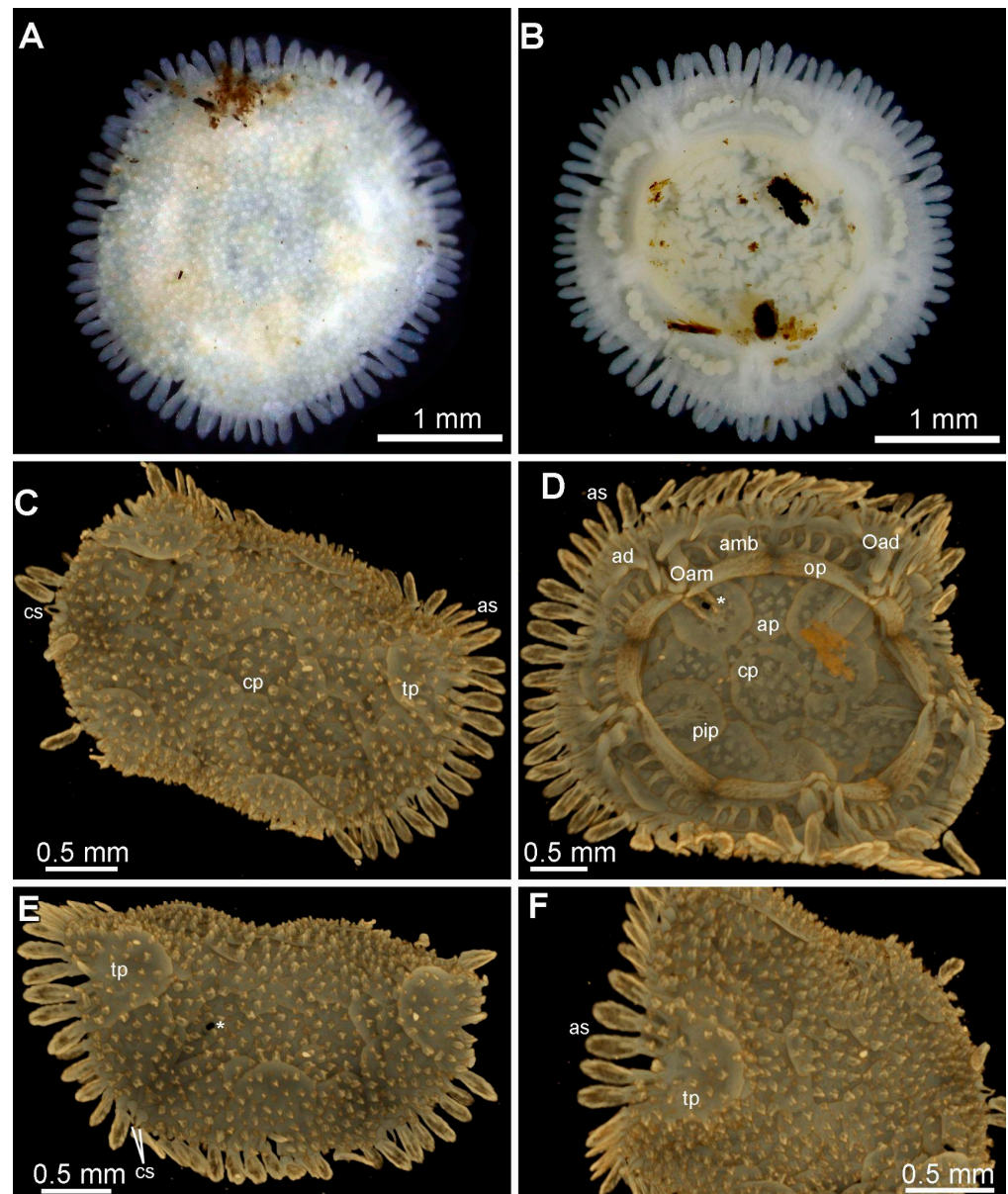


Figure 8. Light-microscopy and μ CT scans of preserved *Xyloplax princealberti* n. sp. specimen collected from a natural wood fall at the Alarcón Rise, Gulf of California, Mexico (paratype SMF 6936). (A) Abactinal view, with wood debris. (B) Actinal view, with wood debris. (C) Abactinal view, μ CT. (D) Actinal view showing abactinal plates. The hydropore is visible. (E) Lateral view showing the hydropore. (F) Lateral view showing the terminal plate and adambulacral spines. Note that the specimen was slightly folded when preserved, which is reflected in the μ CT scans. * indicates hydropore. Legend: **ad**: adambulacral plate; **ap**: abactinal plate; **as**: adambulacral spine; **cp**: centrodorsal plate; **cs**: cygnoid spinelets; **Oad**: oldest (first) adambulacral plate; **Oam**: oldest (first) ambulacral plate; **op**: oral plate; **pip**: primary inter-radial plate; **tp**: terminal plate.

Table 1. Comparative summary of *Xyloplax* characteristics. Comparisons are for 3 mm diameter specimens.

	<i>X. princealberti</i> n. sp.	<i>X. janetae</i>	<i>X. medusiformis</i>	<i>X. turnerae</i>
Abactinal spine base	Round	Rounded to polygonal	Stellate/jagged edges	Stellate/jagged edges
Abactinal spine size range	Uniform, short	Uniform, long	Uniform, long	Bimodal
Adambulacral spines per plate	2–3	3	2	3
Total adambulacral spines	>100	70	50	80–100
Tube feet per segment	10	7	9	11–13
Tube foot shape	Round-bulbous	Round-bulbous	Papillate	Round-bulbous
Terminal plate shape	Badge-shape	Rounded	Square	Badge-shape
Gut expression	Gut absent	Gut absent	Gut absent	Residual gut present
Sexual mode	Hermaphrodite	Gonochoric	Gonochoric	Gonochoric
Developmental mode	“Viviparous”	“Viviparous”	“Viviparous”	Oviparous?
Occurrence	Eastern Pacific (Canada–Costa Rica)	Northeastern Pacific (Oregon)	South Pacific (New Zealand)	Atlantic (Bahamas)
Depth (m)	1845–2421	2675	1057–1208	2066

3.9. Etymology

This species honors His Serene Highness Prince Albert II of Monaco for his efforts to protect the marine environment through the Prince Albert II of Monaco Foundation.

3.10. Remarks

A summary of characters showing *Xyloplax princealberti* n. sp. relative to other known *Xyloplax* species is shown in Table 1. Specimens of *Xyloplax princealberti* n. sp. from Canada to Costa Rica are easily distinguished by their uniformly sized, very short abactinal spinelets. In contrast, *X. janetae* shows elongate spines that rise well above the plane of the disk surface [3]. *Xyloplax medusiformis* appears to share similar types (i.e., uniform) of abactinal spinelets with *X. princealberti* n. sp., but its adambulacral spines, and those of the two other *Xyloplax* species, are more elongated. The adambulacral spines of *X. princealberti* n. sp. also show much more weakly developed serrations, i.e., with smaller shorter points, along the lateral edge of each spine. The terminal plate in *Xyloplax princealberti* n. sp. most resembles the terminal plate of *Xyloplax turnerae*, both displaying a badge-like shape with rounded edges with two distal lobes. Tube foot number per individual adambulacral “segment” varies among the species. *Xyloplax princealberti* n. sp. displays 10 per segment, like *X. medusiformis*, which displays 9, and *Xyloplax janetae*, which shows 7 to 10 tube feet. In contrast, the Atlantic *Xyloplax turnerae* shows 11 to 13 tube feet per adambulacral segment. The simultaneous hermaphroditism observed here in *X. princealberti* n. sp. is a newly observed reproductive strategy for *Xyloplax* but does need further investigation. *Xyloplax turnerae* and *X. medusiformis* were described to be gonochoric [1,2], as evidenced by the visible protrusion of the gonoduct and presence of the cygnoid spinelets in testes-bearing individuals. Though the gonoduct and cygnoid spinelets were not observed in *X. janetae*, this species was presumed to be gonochoric due to the presence of kidney-shaped organs resembling testes in some individuals, but not in those bearing oocytes [4]. *Xyloplax princealberti* n. sp. does possess cygnoid spinelets. The relatively high intraspecific divergence for COI found here within *Xyloplax princealberti* n. sp. (Figure 2A,B) does raise the possibility of a cryptic species complex (see Discussion, Section 4).

In 2011, Gale [29] proposed that a new genus, *Ankyloplax*, should be applied to *X. janetae* based on his interpretation of skeletal morphology that the oral and circumoral ossicles were fused along the length of the oral apophysis as adambulacrals that did not articulate with the adambulacrals. Inspection of *X. janetae* and the type species, *X. medusiformis*, does not agree with Gale’s interpretation. The morphology of both species does not conform to the morphology of his “favoured interpretation” as outlined in Gale (2011: Text Figure 33B from [29]). Similarly, observations of both species do show that

ambulacrals and adambulacrals do articulate, contrary to Gale's conclusion. *Ankyloplax* cannot be confirmed based on its defining characteristics and therefore it is argued to be a synonym of *Xyloplax*.

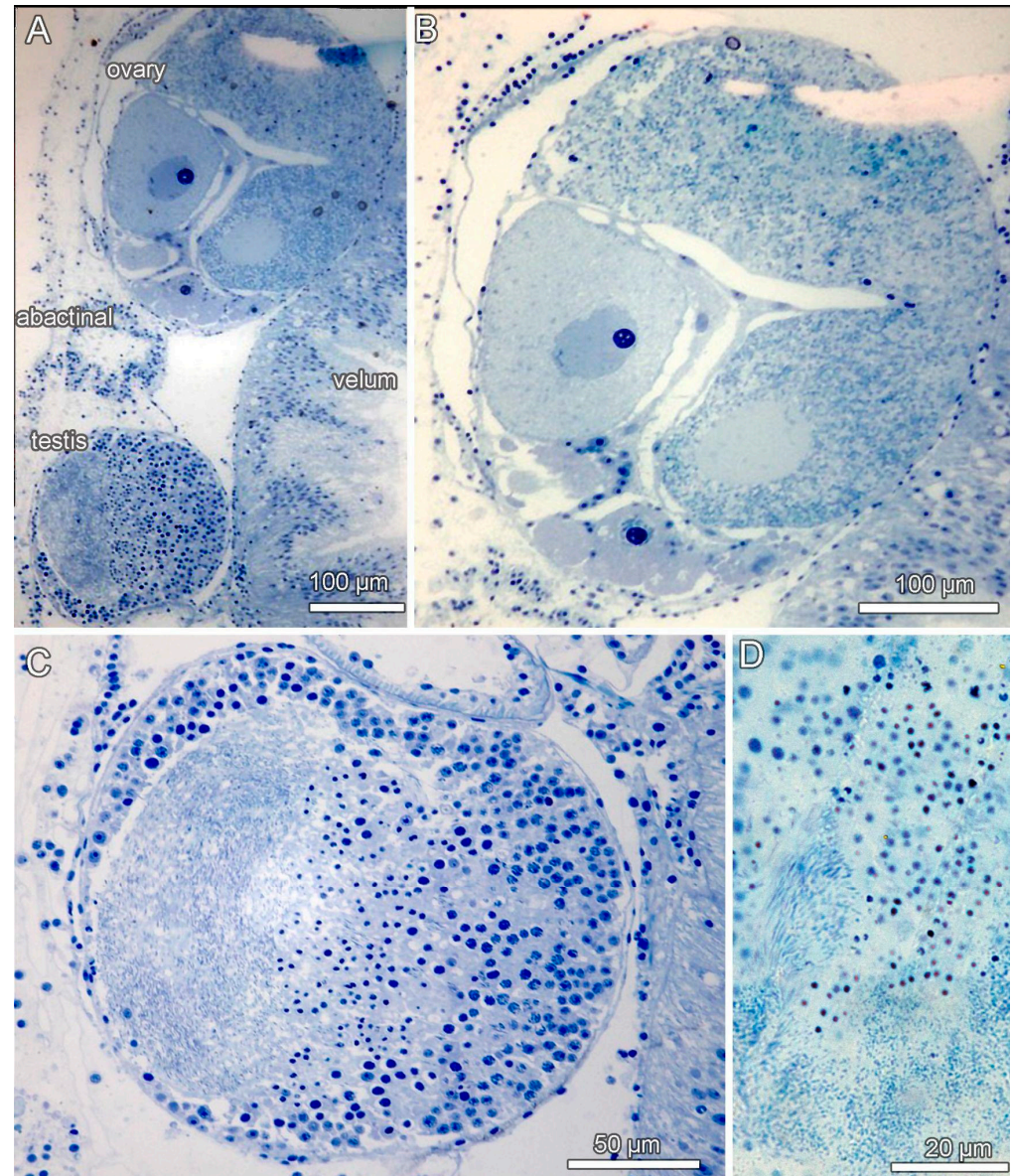


Figure 9. Histology of preserved *Xyloplax princealberti* n. sp. specimen collected from the wood deployment in Juan de Fuca Ridge, offshore Canada (paratype SIO-BIC E11155). (A) A 1 µm semithin section through an ovary with developing oocytes and a testis with developing sperm. (B) Closeup of the ovary, showing at least four developing oocytes. (C) Closeup of the testis, showing various stages of spermiogenesis. (D) Closeup of the testis, showing elongate headed spermatids and sperm.

4. Discussion

The molecular divergence and novel morphology, ecology, and reproductive strategy of the *Xyloplax* collected along the western Pacific coast of North and Central America for this study supports a previously undescribed species: *Xyloplax princealberti* n. sp. COI sequences were only available for one other *Xyloplax* species, *X. janetae*. The minimum COI divergence of 13.5% between *X. janetae* and *X. princealberti* n. sp. reflects reported mean asteroid and echinoderm congeneric COI divergence (on average 15.33%) [30,31]. The 3.3% maximum intraspecific divergence we report here for *Xyloplax princealberti* n. sp.

is much greater than the mean intraspecific divergence of 0.62% previously reported across echinoderms and corresponds to what have been regarded as cryptic species complexes in ophiuroids and crinoids [31,32]. While the intraspecific variation also matches geographic distribution, the consistent morphology of *X. princealberti* n. sp. across its range suggests that further study is needed before splitting the species. If this is achieved, then the southern records would become a new *Xyloplax* species since the type locality is off Canada.

Despite insufficient molecular data to resolve relationships within *Xyloplax*, the known morphologies and type localities of the three other described *Xyloplax* species can be used to infer relationships. Using the original morphological descriptions of these species (summarized in Table 1), *X. janetae* and *X. turnerae* share more morphological characters with *X. princealberti* n. sp. than *X. medusififormis*. *Xyloplax medusififormis* has only been collected from the southwestern Pacific Ocean (Tasman Sea) off the west coast of the South Island of New Zealand [1]. *Xyloplax turnerae* has only been collected from the western North Atlantic Ocean off the east coast of the Andros Island of the Bahamas [2]. *Xyloplax janetae* is geographically closest to *X. princealberti* n. sp. collections; it has only been collected from the northeastern Pacific Ocean off the east coast of Oregon, US, just several hundred miles south of the Juan de Fuca Ridge. Together, the close type locality and similar morphology of *X. janetae* make it the most likely sister species. However, the lack of reliable molecular data for two of the three described *Xyloplax* species makes accurately placing *X. princealberti* n. sp. within *Xyloplax* difficult; therefore, efforts to sequence *X. medusififormis* and *X. turnerae* must be made before interspecific relationships can be defined with certainty.

The gene order of the *X. princealberti* n. sp. mitochondrial genome is consistent with the pattern observed in all other available Asterozoa mitochondrial genomes [24]. Until recently, only ATG and GTG were recognized as start codons in the echinoderm mitochondrial code. However, Quek et al. [24] also identified ATT and ATC as start codons in other Asterozoa, expanding the number of echinoderm start codons to four. Furthermore, their data suggest that TTG could be an alternative start codon for *ND1* and *ND3* in *Euretaster insignis*, consistent with its use in other invertebrates [13,33]. Our results also show that TTG is the start codon for *ND4L* and *ND1* in *Xyloplax*. Accepting that both *Xyloplax* and *Euretaster* belong to Velatida, this indicates a lineage-specific use of the start codon TTG within Asterozoa. The assembled length of the mitogenome of *X. princealberti* n. sp. was 19,663 bp, which is about 3000 bp longer than typically found in Asterozoa [25]. The protein-coding genes, *rRNA* and *tRNA* genes, were all of the usual length, and the extra length was restricted to the non-coding control region. It is possible that our assembly was artefactual with regard to the non-coding region and further sequencing may be required to resolve this. Our raw reads are publicly available so that alternative assembly methods can be attempted (GenBank = PRJNA1032079).

The analysis of the mitochondrial genome of *X. princealberti* n. sp. in relation to other asterozoans provided two results depending on whether the protein-coding genes were coded as DNA (Figure 3) or as amino acids (Figure S1). *Xyloplax princealberti* n. sp. either formed a clade with the two members of Velatida included, forming the sister group to the rest of Asterozoa (Figure 3), or it formed a grade with the two members of Velatida, with *X. princealberti* n. sp. as sister group to Asterozoa (Figure S1). While a relationship with Velatida has been shown with an analysis of the transcriptome of *X. princealberti* n. sp. [8], that study determined Velatida to be further nested within Asterozoa.

This study expands the range of *Xyloplax* to the tropical eastern Pacific. *Xyloplax* has now been recorded from several localities throughout the North Pacific Ocean. This suggests that *Xyloplax* is more ubiquitous than previously believed, and that its elusiveness is a byproduct of sampling efforts to date. This study also records the first observation of *Xyloplax* residing in *Ridgeia piscesae* tubeworm bushes, which is somewhat remarkable since the fauna of the Juan de Fuca vents have seemingly been well studied [34].

A normal gut is absent in all *Xyloplax* species except for a “residual” sac-like gut found in *X. turnerae* [1–3]. Baker et al. [2] proposed that “the ventral velum of *Xyloplax* derived from the stretching of a simple, sac-like stomach from its original internal position, by

opening of the oral frame. Thus, the outer surface of the velum is formed from the inner lining of the stomach." This hypothesis has yet to be assessed. Nichols [35] speculated that there may be a form of symbiosis occurring between *Xyloplax* and bacteria on the wood surface. The discovery of *Xyloplax* living in a bacteria-rich environment at a hydrothermal vent implies that the diet of *Xyloplax* is not wood-dependent. Whether *Xyloplax* consumes bacteria directly or has a form of symbiosis with them requires further investigation.

Supplementary Materials: The following supporting information can be downloaded at: <https://www.mdpi.com/article/10.3390/d15121212/s1>, Figure S1: Maximum likelihood phylogeny built from the 15 gene dataset with 13 protein coding genes coded as amino acids and the two RNA gene partitions encoded as DNA.; Figure S2: Micro-CT surface rendering video of the cybertype of *Xyloplax princealberti* n. sp. collected from a natural woodfall at the Alarcón Rise, Gulf of California, Mexico (SMF 6936).

Author Contributions: Conceptualization, G.W.R.; methodology, G.W.R., C.Y.P., J.S., E.T. and A.S.H.; validation, G.W.R. and C.L.M.; formal analysis, G.W.R., C.L.M., E.T., C.Y.P., J.S., R.E.B.-R. and A.S.H.; investigation, G.W.R., C.Y.P., C.L.M., R.E.B.-R., A.G., B.M.G., E.T. and A.S.H.; resources, G.W.R. and E.T.; data curation, G.W.R., C.Y.P. and E.T.; writing—original draft preparation, G.W.R., C.Y.P., C.L.M. and E.T.; visualization, G.W.R. and E.T.; supervision, G.W.R.; project administration, G.W.R.; funding acquisition, G.W.R. All authors have read and agreed to the published version of the manuscript.

Funding: This research was funded by the U.S. National Science Foundation (NSF) grant OCE-1634172. R. Boschen-Rose was supported by a Canadian Healthy Oceans Network II (CHONeII) post-doctoral fellowship at University of Victoria. Cruise PAC2016-26 on CCGS *Tully* was jointly funded by Fisheries and Oceans Canada (DFO), CHONeII, University of Victoria, and Memorial University.

Institutional Review Board Statement: Not applicable.

Data Availability Statement: COI sequences, genome skimming data, and the mitogenome are all deposited in GenBank. The raw microCT dataset, together with the surface renderings, are deposited online as a cybertype: <https://doi.org/10.5281/zenodo.10042987> (accessed 26 October 2023).

Acknowledgments: We would like to thank the captains and crews of the RV *Atlantis* and DSV *Alvin*, R/V *Western Flyer*, and ROV *Doc Ricketts*, CCGS *Tully*, and ROV *ROPOS* and the scientists involved with sample collection. We thank Verena Tunnicliffe, Dave Clague, and Lisa Levin for leading cruises that obtained these samples or deploying wood that provided specimens. Mexican specimens were collected under a permit to the Monterey Bay Aquarium and Research Institute. Costa Rica specimens were collected under the following permits issued by CONAGEBIO (Comisión Nacional para la Gestión de la Biodiversidad) and SINAC (Sistema Nacional de Áreas de Conservación) under MINAE (Ministerio de Ambiente y Energía), Government of Costa Rica: SINAC- CUSBSE-PI-R-032-2018 and the Contract for the Grant of Prior Informed Consent between MINAE-SINAC-ACMC and Jorge Cortés Nuñez for the Basic Research Project "Cuantificación de los vínculos biológicos, químicos y físicos entre las comunidades quimiosintéticas con el mar profundo circundante". We thank HMWK (Hessian Ministry of Science and Arts) through the IWB-EFRE program, Project number: 20009100, and SOSA (Senckenberg Ocean Species Alliance) for financing the Werth μ CT scanner under the project title "3D-Forschung mittels hochauflösender μ CT für den digitalen Zwilling von Objekten". Special thanks to Charlotte Seid for careful work in cataloging the samples and Dakota Betz for a final DNA sequence.

Conflicts of Interest: The authors declare no conflict of interest. The funders had no role in the design of the study; in the collection, analyses, or interpretation of data; in the writing of the manuscript; or in the decision to publish the results.

References

1. Baker, A.N.; Rowe, F.W.E.; Clark, H.E.S. A New Class of Echinodermata from New Zealand. *Nature* **1986**, *321*, 862–864. [[CrossRef](#)]
2. Rowe, F.W.E.; Baker, A.N.; Clark, H.E.S. The Morphology, Development and Taxonomic Status of *Xyloplax* Baker, Rowe and Clark (1986) (Echinodermata: Concentricycloidea), with the Description of a New Species. *Proc. R. Soc. Lond.* **1988**, *233*, 431–459. [[CrossRef](#)]
3. Mah, C.L. A New Species of *Xyloplax* (Echinodermata:Asteroidea:Concentricycloidea) from the Northeast Pacific: Comparative Morphology and a Reassessment of Phylogeny. *Invertebr. Biol.* **2006**, *125*, 136–153. [[CrossRef](#)]
4. Voight, J.R. First Report of the Enigmatic Echinoderm *Xyloplax* from the North Pacific. *Biol. Bull.* **2005**, *208*, 77–80. [[CrossRef](#)]

5. Smith, A.B. To Group or Not to Group: The Taxonomic Position of *Xyloplax*. In *Echinoderm Biology: Proceedings of the Sixth International Echinoderm Conference*; Burke, R.D., Mladenov, P.V., Lambert, P., Parsley, R.L., Eds.; A. A. Balkema: Rotterdam, The Netherlands, 1988; pp. 17–23.
6. Pearse, V.; Pearse, J. Echinoderm Phylogeny and the Place of Concentricycloids. In *Echinoderms through Time (Echinoderms, Dijon)*; David, B., Guille, A., Feral, J.-P., Roux, M., Eds.; Balkema: Rotterdam, The Netherlands, 1994; pp. 121–126.
7. Janies, D.A.; Voight, J.R.; Daly, M. Echinoderm Phylogeny Including *Xyloplax*, a Progenetic Asteroid. *Syst. Biol.* **2011**, *60*, 420–438. [[CrossRef](#)]
8. Linchangco, G.V., Jr.; Foltz, D.W.; Reid, R.; Williams, J.; Nodzak, C.; Kerr, A.M.; Miller, A.K.; Hunter, R.; Wilson, N.G.; Nielsen, W.J.; et al. The Phylogeny of Extant Starfish (Asteroidea: Echinodermata) Including *Xyloplax*, Based on Comparative Transcriptomics. *Mol. Phylogenet. Evol.* **2017**, *115*, 161–170. [[CrossRef](#)]
9. Folmer, O.; Black, M.; Hoeh, W.; Lutz, R.; Vrijenhoek, R. DNA Primers for Amplification of Mitochondrial Cytochrome c Oxidase Subunit I from Diverse Metazoan Invertebrates. *Mol. Mar. Biol. Biotechnol.* **1994**, *3*, 294–299.
10. Jin, J.-J.; Yu, W.-B.; Yang, J.-B.; Song, Y.; dePamphilis, C.W.; Yi, T.-S.; Li, D.-Z. GetOrganelle: A Fast and Versatile Toolkit for Accurate de Novo Assembly of Organelle Genomes. *Genome Biol.* **2020**, *21*, 241. [[CrossRef](#)]
11. Langmead, B.; Salzberg, S.L. Fast Gapped-Read Alignment with Bowtie 2. *Nat. Methods* **2012**, *9*, 357–359. [[CrossRef](#)]
12. Bankevich, A.; Nurk, S.; Antipov, D.; Gurevich, A.A.; Dvorkin, M.; Kulikov, A.S.; Lesin, V.M.; Nikolenko, S.I.; Pham, S.; Pribelski, A.D.; et al. SPAdes: A New Genome Assembly Algorithm and Its Applications to Single-Cell Sequencing. *J. Comput. Biol.* **2012**, *19*, 455–477. [[CrossRef](#)]
13. Donath, A.; Jühling, F.; Al-Arab, M.; Bernhart, S.H.; Reinhardt, F.; Stadler, P.F.; Middendorf, M.; Bernt, M. Improved Annotation of Protein-Coding Genes Boundaries in Metazoan Mitochondrial Genomes. *Nucleic Acids Res.* **2019**, *47*, 10543–10552. [[CrossRef](#)]
14. Bolger, A.M.; Lohse, M.; Usadel, B. Trimmomatic: A Flexible Trimmer for Illumina Sequence Data. *Bioinformatics* **2014**, *30*, 2114–2120. [[CrossRef](#)]
15. Grabherr, M.G.; Haas, B.J.; Yassour, M.; Levin, J.Z.; Thompson, D.A.; Amit, I.; Adiconis, X.; Fan, L.; Raychowdhury, R.; Zeng, Q.; et al. Full-Length Transcriptome Assembly from RNA-Seq Data without a Reference Genome. *Nat. Biotechnol.* **2011**, *29*, 644–652. [[CrossRef](#)] [[PubMed](#)]
16. Maddison, W.P.; Maddison, D.R. Mesquite: A Modular System for Evolutionary Analysis. Version 3.5. 2018. Available online: <http://www.mesquiteproject.org> (accessed on 15 January 2023).
17. Katoh, K.; Standley, D.M. MAFFT Multiple Sequence Alignment Software Version 7: Improvements in Performance and Usability. *Mol. Biol. Evol.* **2013**, *30*, 772–780. [[CrossRef](#)] [[PubMed](#)]
18. Edler, D.; Klein, J.; Antonelli, A.; Silvestro, D. RaxmlGUI 2.0: A Graphical Interface and Toolkit for Phylogenetic Analyses Using RAxML. *Methods Ecol. Evol.* **2021**, *12*, 373–377. [[CrossRef](#)]
19. Kozlov, A.M.; Darriba, D.; Flouri, T.; Morel, B.; Stamatakis, A. RAxML-NG: A Fast, Scalable and User-Friendly Tool for Maximum Likelihood Phylogenetic Inference. *Bioinformatics* **2019**, *35*, 4453–4455. [[CrossRef](#)] [[PubMed](#)]
20. Darriba, D.; Posada, D.; Kozlov, A.M.; Stamatakis, A.; Morel, B.; Flouri, T. ModelTest-NG: A New and Scalable Tool for the Selection of DNA and Protein Evolutionary Models. *Mol. Biol. Evol.* **2020**, *37*, 291–294. [[CrossRef](#)]
21. Swofford, D.L. *PAUP*. Phylogenetic Analysis Using Parsimony (*and Other Methods)*; Version 4; Sinauer Associates: Sunderland, MA, USA, 2002.
22. Clement, M.; Posada, D.; Crandall, K.A. TCS: A Computer Program to Estimate Gene Genealogies. *Mol. Ecol.* **2000**, *9*, 1657–1659. [[CrossRef](#)]
23. Leigh, J.W.; Bryant, D. POPART: Full-Feature Software for Haplotype Network Construction. *Methods Ecol. Evol.* **2015**, *6*, 1110–1116. [[CrossRef](#)]
24. Quek, Z.B.R.; Chang, J.J.M.; Ip, Y.C.A.; Chan, Y.K.S.; Huang, D. Mitogenomes Reveal Alternative Initiation Codons and Lineage-Specific Gene Order Conservation in Echinoderms. *Mol. Biol. Evol.* **2021**, *38*, 981–985. [[CrossRef](#)]
25. Sun, S.; Xiao, N.; Sha, Z. Mitogenomics Provides New Insights into the Phylogenetic Relationships and Evolutionary History of Deep-Sea Sea Stars (Asteroidea). *Sci. Rep.* **2022**, *12*, 4656. [[CrossRef](#)]
26. Shimodaira, H. An Approximately Unbiased Test of Phylogenetic Tree Selection. *Syst. Biol.* **2002**, *51*, 492–508. [[CrossRef](#)]
27. Nguyen, L.-T.; Schmidt, H.A.; von Haeseler, A.; Minh, B.Q. IQ-TREE: A Fast and Effective Stochastic Algorithm for Estimating Maximum-Likelihood Phylogenies. *Mol. Biol. Evol.* **2015**, *32*, 268–274. [[CrossRef](#)] [[PubMed](#)]
28. Limaye, A. Drishti: A Volume Exploration and Presentation Tool. In Proceedings of the Developments in X-ray Tomography VIII, SPIE, San Diego, CA, USA, 17 October 2012; Volume 8506, pp. 191–199.
29. Gale, A. The Phylogeny of Post-Palaeozoic Asteroidea (Echinodermata, Neoasteroidea). *Spec. Pap. Palaeontol.* **2011**, *85*, 1–112.
30. Hebert, P.D.N.; Cywinska, A.; Ball, S.L.; deWaard, J.R. Biological Identifications through DNA Barcodes. *Proc. Biol. Sci.* **2003**, *270*, 313–321. [[CrossRef](#)] [[PubMed](#)]
31. Ward, R.D.; Holmes, B.H.; O’Hara, T.D. DNA Barcoding Discriminates Echinoderm Species. *Mol. Ecol. Resour.* **2008**, *8*, 1202–1211. [[CrossRef](#)]
32. McLaughlin, E.L.; Wilson, N.G.; Rouse, G.W. Resolving the Taxonomy of the Antarctic Feather Star Species Complex *Promachocri-nus ‘Kerguelensis’* (Echinodermata: Crinoidea). *Invertebr. Syst.* **2023**, *37*, 498–527. [[CrossRef](#)]

33. Okimoto, R.; Macfarlane, J.L.; Wolstenholme, D.R. Evidence for the Frequent Use of TTG as the Translation Initiation Codon of Mitochondrial Protein Genes in the Nematodes, *Ascaris Suum* and *Caenorhabditis Elegans*. *Nucleic Acids Res.* **1990**, *18*, 6113–6118. [[CrossRef](#)]
34. Lelièvre, Y.; Sarrazin, J.; Marticorena, J.; Schaal, G.; Day, T.; Legendre, P.; Hourdez, S.; Matabos, M. Biodiversity and Trophic Ecology of Hydrothermal Vent Fauna Associated with Tubeworm Assemblages on the Juan de Fuca Ridge. *Biogeosciences* **2018**, *15*, 1–34. [[CrossRef](#)]
35. Nichols, D. A New Class of Echinoderms. *Nature* **1986**, *321*, 808. [[CrossRef](#)]

Disclaimer/Publisher’s Note: The statements, opinions and data contained in all publications are solely those of the individual author(s) and contributor(s) and not of MDPI and/or the editor(s). MDPI and/or the editor(s) disclaim responsibility for any injury to people or property resulting from any ideas, methods, instructions or products referred to in the content.